An Intermediate Structure in the Thermal Unfolding of the GTPase Domain of Human Septin 4 (SEPT4/Bradeion-β) Forms Amyloid-like Filaments in Vitro[†]

Wanius Garcia,*[,‡] Ana Paula Ulian de Araújo,[‡] Flávio Lara,[§] Debora Foguel,[||] Manami Tanaka,[⊥] Tomoo Tanaka,[@] and Richard Charles Garratt*[,‡]

Centro de Biotecnologia Molecular e Estrutural, Instituto de Física de São Carlos, Universidade de São Paulo, São Paulo, Brazil, Programa de Biologia Molecular e Celular, Instituto de Bioquímica Médica, Universidade Federal do Rio de Janeiro, Rio de Janeiro 21941-590, Brazil, Programa de Biologia Estrutural, Instituto de Bioquímica Médica, Universidade Federal do Rio de Janeiro, Rio de Janeiro 21941-590, Brazil, National Institute of Advanced Industrial Science and Technology, Higashi, Tsukuba Science City, Ibaraki, Japan, and Tokai University School of Medicine, Isehara, Kanagawa 259-1193, Japan

Received April 13, 2007; Revised Manuscript Received July 25, 2007

ABSTRACT: SEPT4 is a member of the mammalian septin family of GTPases. Mammalian septins are conserved proteins which form heteropolymers in vivo and which are implicated in a variety of cellular functions such as cytokinesis, exocytosis, and vesicle trafficking. However, their structural properties and modes of action are largely unknown. There is a limited, but as yet inconclusive, amount of experimental data suggesting that SEPT4 may accumulate in tau-based filamentous deposits and cytoplasmic inclusions in Alzheimer's and Parkinson's disease, respectively. Here we report an intermediate structure of the GTPase domain of human SEPT4 (SEPT4-G) during unfolding transitions induced by temperature. This partially unfolded intermediate, which is rich in β-sheet and free of bound nucleotide, was plagued by irreversible aggregation. The aggregates have the ability to bind specific dyes such as Congo red and thioflavin-T, suggesting they are amyloid in nature. Under electron microscopy, fibers of variable diameter extending for several micrometers in length can be visualized. This is the first report of amyloid formation by a septin or domain thereof, and the capacity of SEPT4-G to form such fibrillar aggregates may shed some light on the current discussion concerning the formation of homo- and heteropolymers of septins in vitro.

Septins are a family of conserved proteins that form hetero-oligomeric complexes that assemble into filaments (*1*−*3*). Those observed in yeast form filaments of variable length that are 7−9 nm in diameter, although their mechanism of assembly is still unknown (*1*). Similar filaments have also been isolated from *Drosophila* and mammalian brain tissue (*2*, *3*). In vivo, these complexes are always purified in the form of heterofilaments, composed of three or four different septin polypeptides with a defined stoichiometry. These heteromeric polymers are widely believed to be physiologically relevant for septin function, including their role in cytokinesis, exocytosis, cell division, membrane trafficking, etc. Similar filaments can be recovered after coexpression of the appropriate septins in vitro (*4*, *5*). On the other hand, only two reports describe the formation of homopolymers in vitro, and the physiological relevance of these in vivo is questionable (*6*, *7*).

In mammals, 13 mammalian septins have been identified which have been classified according to a standardized nomenclature which has been recently adopted (*8*). The sequences of these proteins can be divided into three domains: a variable N-terminus, a central GTPase domain, and a C-terminal region which generally includes sequences characteristic of coiled coils (*9*). The central GTPase domain is highly conserved with a minimum level of similarity of 70% among septins from the same species (*10*). This is not the case for the N- and C-terminal domains, which vary greatly both within and between species. The GTPase domain is characterized by the presence of a P-loop motif (G1 or Walkers's A box) close to its N-terminus (*11*). Both the binding of GTP and its hydrolysis have been experimentally demonstrated for several septins in vitro (*4*, *6*, *12*, *13*).

SEPT4/Bradeion-β (NCBI accession number NP_004565) is one member of the mammalian septin family (*14*, *15*). As with many other septins, human SEPT4 presents different isoforms and its gene has a significant tissue and adult stage specific expression profile being observed in colorectal and urologic cancer as well as malignant melanoma (*14*, *16*). Furthermore, the impaired expression of the human SEPT4 gene products directly affects cell division and causes selective G2 arrest in cultivated human cancer cells (*17*).

[†] This work was supported by FAPESP via a grant to the Centro de Biotecnologia Molecular Estrutural (98/14138-2) and by CNPq via the Instituto Milênio de Biologia Estrutural em Biomedicina e Biotecnologia.

* To whom correspondence should be addressed: Instituto de Física de São Carlos, Universidade de São Paulo (USP), Av. Trabalhador São-carlense, 400, 13560250, São Carlos (SP), Brazil. Telephone: (16) 33739874. Fax: (16) 33739881. E-mail: wanius@if.sc.usp.br, richard@if.sc.usp.br.

[‡] Universidade de São Paulo.

[§] Programa de Biologia Molecular e Celular, Instituto de Bioquímica Médica, Universidade Federal do Rio de Janeiro.

[||] Programa de Biologia Estrutural, Instituto de Bioquímica Médica, Universidade Federal do Rio de Janeiro.

[⊥] National Institute of Advanced Industrial Science and Technology.

[@] Tokai University School of Medicine.

10.1021/bi700702w CCC: $37.00
Published on Web 09/01/2007

One report also describes the accumulation of human SEPT4 in tau-based filamentous deposits known as neurofibrillary tangles and glial fibrils in Alzheimer's disease (*18*). A second paper reported that human SEPT4 is also involved in the formation of cytoplasmic inclusions in Parkinson's disease as well as in the induction of cell death (*19*).

It is now known that many neurodegenerative diseases arise from abnormal protein interaction in the central nervous system. In many cases, there are characteristic deposits of protein aggregates in the brain, which can be cytoplasmic, nuclear, or extracellular (*20*−*23*). Protein aggregation can result from a mutation in the sequence of the disease-related protein, a genetic alteration that causes an elevation in the amounts of a normal protein, or can occur in the absence of genetic alterations, perhaps triggered by environmental stress or aging (*24*). In aggregation diseases, large intracellular or extracellular accumulations of aggregated protein, known as inclusion bodies, are often formed. The inclusion bodies frequently contain the disease protein in a fibrillar aggregated form called amyloid (*25*, *26*), which also may contain other material.

In an attempt to better characterize the SEPT4 molecule in structural terms, we have recently described its molecular dissection, with the intention of generating more readily crystallizable protein products (*27*). With this and the need to better characterize the stability of the individual domains in mind, this study describes the analysis of the structural integrity of the GTPase domain of human SEPT4 (SEPT4-G) using circular dichroism spectroscopy (CD), right-angle light scattering, dynamic light scattering (DLS), and the use of the fluorescent probes 1-anilinonaphthalene-8-sulfonate (ANS) and thioflavin-T (ThT). We demonstrate an intermediate structure, rich in β-sheet, present during the thermal unfolding of SEPT4-G. This intermediate has a tendency to form aggregates and binds ThT and Congo red, suggesting the formation of amyloid-like aggregates. The presence of large organized structures was subsequently directly observed by electron microscopy.

A better understanding of the biochemistry and biophysics of the processes of conformational change and aggregation of septins will be crucial to unraveling their involvement in cellular toxic events and cellular protective mechanisms as well as aiding in the understanding of their tendency to aggregate in vitro. In addition, these intermediates may be targets for the development of lead compounds capable of their disruption.

MATERIALS AND METHODS

Materials. The pET28a(+) bacterial expression vector and Ni-NTA resin were purchased from Novagen. Superdex-200 resin was purchased from Amersham Pharmacia Biotech (GE Healthcare). Guanosine 5′-triphosphate (GTP), protein standards used as SDS−PAGE markers, Congo red, ANS, and ThT were purchased from Sigma. All other chemicals were of analytical grade (Sigma, Amersham).

Expression and Purification of the Recombinant GTPase Domain of Human SEPT4 (SEPT4-G). The GTPase domain of human SEPT4 (SEPT4-G, residues 144−416) was used for this study because of its higher solubility, its higher expression level, and its greater stability when compared with those of full-length SEPT4 (*27*). The expression and purification of SEPT4-G were carried out as described previously (*27*) with slight modifications, and its purity was checked by SDS−PAGE. SEPT4-G was purified with or without the addition of GTP to the purification buffer system. The SEPT4-G concentration, in all cases, was determined from its absorbance at 280 nm in 6.0 M urea using a theoretical extinction coefficient (21 980 M^{-1} cm^{-1}) based on its amino acid composition (*28*), employing a U-2001 Hitachi UV−visible spectrophotometer. The nucleotide content was estimated using the method described by Seckler (*29*). For right-angle light scattering and ThT fluorescence experiments, the full SEPT4 molecule and the SEPT4-GC product (the GTPase domain together with the C-terminal domain) were expressed and purified as described previously (*27*).

Size Exclusion Chromatography (SEC). SEPT4-G was initially purified in the absence of GTP. After affinity purification, samples of SEPT4-G were prepared in buffer containing 25 mM Tris-HCl, 20 mM NaCl, and 5% glycerol (pH 7.8) with or without GTP at a final concentration of 100 μM. Subsequently, each sample was filtered by SEC on a Superdex-200 column coupled to a HPLC system at 4 °C, eluted with the same buffer (without GTP) at a flow rate of 0.5 mL/min, monitored by absorbance at both 280 and 254 nm, and collected in 1 mL fractions. Subsequent to these experiments, all further purifications of SEPT4-G were performed in the presence of GTP in all the buffers.

Circular Dichroism (CD) Spectroscopy. Thermal unfolding of SEPT4-G was monitored by far-UV CD spectroscopy (over a wavelength range of 200−250 nm) using a J-715 Jasco spectropolarimeter equipped with a temperature control. CD spectra were measured from samples in 1 mm path length quartz cuvettes and were the average of 16 accumulations, using a scanning speed of 20 nm/min, a spectral bandwidth of 1 nm, and a response time of 1 s. The SEPT4-G concentration was approximately 9 μM in 25 mM Tris-HCl, 20 mM NaCl, 0.1 mM EDTA, and 5% glycerol (pH 7.8). All spectra were smoothed by Fourier filtering using the FFT option of Origin 7.0 prior to subsequent analysis.

Thermal denaturation of SEPT4-G was characterized by measuring the ellipticity changes at 221 nm induced by a temperature increase from 6 to 70 °C at a heating rate of 10 °C/h. Specifically, the temperature of the sample was increased by 2 °C over a period of 2 min followed by a rest period of a further 2 min. Subsequently, 16 data acquisition scans were recorded, each of which took 30 s, leading to a total of 12 min per data point. CD spectra were obtained on a degree ellipticity scale. The buffer contribution was subtracted in all of the experiments. The ellipticity data obtained from the study of thermal denaturation were analyzed assuming that this is an irreversible transition process. Deconvolution of the spectrum was performed using the K2d algorithm (http://www.embl-heidelberg.de/~andrade/k2d/).

Right-Angle Light Scattering. SEPT4-G (4 μM) in 25 mM Tris-HCl, 20 mM NaCl, 0.1 mM EDTA, 5% glycerol buffer (pH 7.8) was centrifuged (16000*g* for 15 min at 4 °C) and placed in a 0.5 cm path length quartz cuvette in a steady-state spectrofluorimeter, model K2 ISS, equipped with a refrigerated circulator. The sample was illuminated with 350 nm light, and the scattering at the same wavelength was collected at an angle of 90°. Measurements were taken at

20, 30, 34, 37, and 40 °C. All intensity measurements are given in arbitrary units after subtraction of the light scattering by the buffer. Identical experiments were performed at 20 and 37 °C using the whole SEPT4 and SEPT4-GC at a concentration of 4 μM in 25 mM Tris-HCl, 20 mM NaCl, 0.1 mM EDTA, 5% glycerol buffer (pH 7.8).

Nucleotide Release. Samples of SEPT4-G at a concentration of 20 μM in 25 mM Tris-HCl, 20 mM NaCl, 0.1 mM EDTA, 5% glycerol buffer (pH 7.8) were incubated at 4, 18, 24, and 37 °C for 90 min and subsequently centrifuged (at 4 °C) using Millipore concentrators (10 kDa cutoff). The absorption spectrum of the filtrate was measured from 240 to 330 nm using a U-2001 Hitachi UV−visible spectrophotometer to assess its nucleotide content.

Binding of Congo Red to SEPT4-G. Samples of SEPT4-G ($\sim$10 μM) were incubated at 37 °C for 1 h and subsequently stained with a 10 mM Congo red solution in 25 mM Tris-HCl (pH 7.8), 20 mM NaCl, and 5% glycerol for a further hour. Each sample was washed several times with the same buffer. Subsequently, the sample was observed under bright field and between crossed polars utilizing a Zeiss Axioplan 2 microscope.

ANS Fluorescence Assay. SEPT4-G was at 15 μM in 25 mM Tris-HCl, 20 mM NaCl, 0.1 mM EDTA, 5% glycerol buffer (pH 7.8) and ANS at a final concentration of 150 μM. Fluorescence emission was measured within the range of 400−600 nm, after excitation at 360 nm within a temperature range from 6 to 70 °C at a heating rate of 10 °C/h.

Thioflavin-T Fluorescence Assay. SEPT4-G at 10 μM in 25 mM Tris-HCl, 20 mM NaCl, 0.1 mM EDTA, 5% glycerol buffer (pH 7.8) was used in this experiment. SEPT4-G was incubated with 60 μM ThT, and the excitation wavelength was 450 nm and the emission measured at 482 nm. Measurements were taken at 20, 30, 37, and 40 °C. The emission was collected for a period of 1 h. In a second experiment which included temperatures above 45 °C, the samples were incubated for 1 h at the appropriate temperature and subsequently cooled to room temperature prior to the addition of 60 μM ThT, and the fluorescence intensity was measured as described above. Identical experiments with ThT were performed at 20 and 37 °C using the full SEPT4 molecule and SEPT4-GC at a concentration of 10 μM using the same buffer and conditions employed for the SEPT4-G experiments.

Dynamic Light Scattering (DLS). SEPT4-G eluted in peaks 1 and 2 [purification without GTP in 25 mM Tris-HCl, 20 mM NaCl, 0.1 mM EDTA, 5% glycerol buffer (pH 7.8)] was centrifuged at 14000*g* for 10 min at 4 °C and immediately loaded into quartz cuvetttes prior to measurement. DLS was performed using a DynaPro Molecular Sizing instrument, with DYNAMICS control and analysis software (DYNAMICS version 5, Proteins Solutions, Inc.). Data collection times of 2 s were used for a minimum of 60 acquisitions.

Electron Microscopy. SEPT4-G was incubated at 37 °C for 30 min in buffer containing 25 mM Tris-HCl, 20 mM NaCl, 5% glycerol buffer (pH 7.8). Negative staining was performed by appling to glow-discharged carbon-coated grids for 1 min. The grids were stained with filtered 1% uranyl acetate for 1 min and subsequently washed with the same buffer. Images were acquired in a Morgagni (Fei/Philips) transmission electron microscope working at 80 kV.

RESULTS AND DISCUSSION

SEPT4-G Has a Tendency To Form Aggregates in the Absence of GTP. To apply biophysical techniques to the study of the stability of purified septins, it was initially necessary to establish efficient expression protocols for the production of soluble protein products. In this study, we have concentrated on the GTPase domain of SEPT4 (SEPT4-G) as it can be readily expressed in stable form in *Escherichia coli* (*27*). Initial attempts to express the protein in the absence of GTP in the lysis buffer yielded two principal peaks, both of which correspond to SEPT4-G on SDS−PAGE (Figure 1A,B). The first peak eluted in the void volume of the Superdex-200 column, was free of bound nucleotide, and corresponded to high-molecular weight aggregates corresponding to particles with a mean hydrodynamic radius of approximately 30 nm (Figure 2B). The second peak, on the other hand, corresponded to a monodisperse dimer in solution with a hydrodynamic radius of 4.0 $\pm$ 0.3 nm (Figure 2A) and was shown to have nucleotide bound (0.7 $\pm$ 0.1 nucleotide per monomer). If this sample is then incubated at 37 °C for 1 h and subsequently analyzed by DLS, a profile similar to that seen in Figure 2B is once more observed.

These results suggest there is a correlation between protein aggregation and nucleotide content on heterologous expression. Indeed, the relative distribution of protein between the two peaks can be altered by adding GTP to the sample after affinity chromatography. This results in an increase in the size of the second peak at the expense of the first (Figure 1A). However, this recovery is not total, indicating that the first peak may be heterogeneous in nature, and it is possible to recover only part of the molecules in the lower-molecular weight fraction. This problem was completely resolved by the addition of GTP during all subsequent purifications, from cell lysis onward. Under these conditions, the first peak disappeared altogether and the preparation ran as a single peak which contained 0.9 $\pm$ 0.1 nucleotide bound per protein monomer (Figure 1C). This is indicative that nucleotide-free SEPT4-G when expressed in *E. coli* is not correctly folded, and that GTP binding aids in its folding and stability, which has been similarly described for *Dictyostelium* elongation factor 1A (*30*). Furthermore, Huang et al. (*7*) have similarly reported the need to include nucleotide for the successful expression of SEPT2 in stable form. Mitchison and Field (*31*) have gone as far as to suggest that GTP may actually trigger GTPase domain folding in the case of SEPT2 from *Xenopus laevis*.

Heat Treatment Induces an α*- to* β*-Transition in SEPT4-G: Formation of an Intermediate Species*. The CD spectrum of purified SEPT4-G is typical of proteins containing elements of α-helical secondary structure which, together with the presence of bound nucleotide, is indicative that the recombinant domain has folded correctly. The deconvolution of this spectrum led to an estimated content of 30% α-helix, 24% β-strand, and 46% turns and irregular structures (*27*). The spectrum remains relatively constant below 20 °C (Figure 3A). This can be readily followed by accompanying the ellipticity at 221 nm, which is the dominant peak characteristic of α-helical structure and falls within a region of the spectrum where the signal-to-noise ratio is of high quality.

The spectral profile is progressively altered, however, when the temperature is increased above 22 °C, with a loss

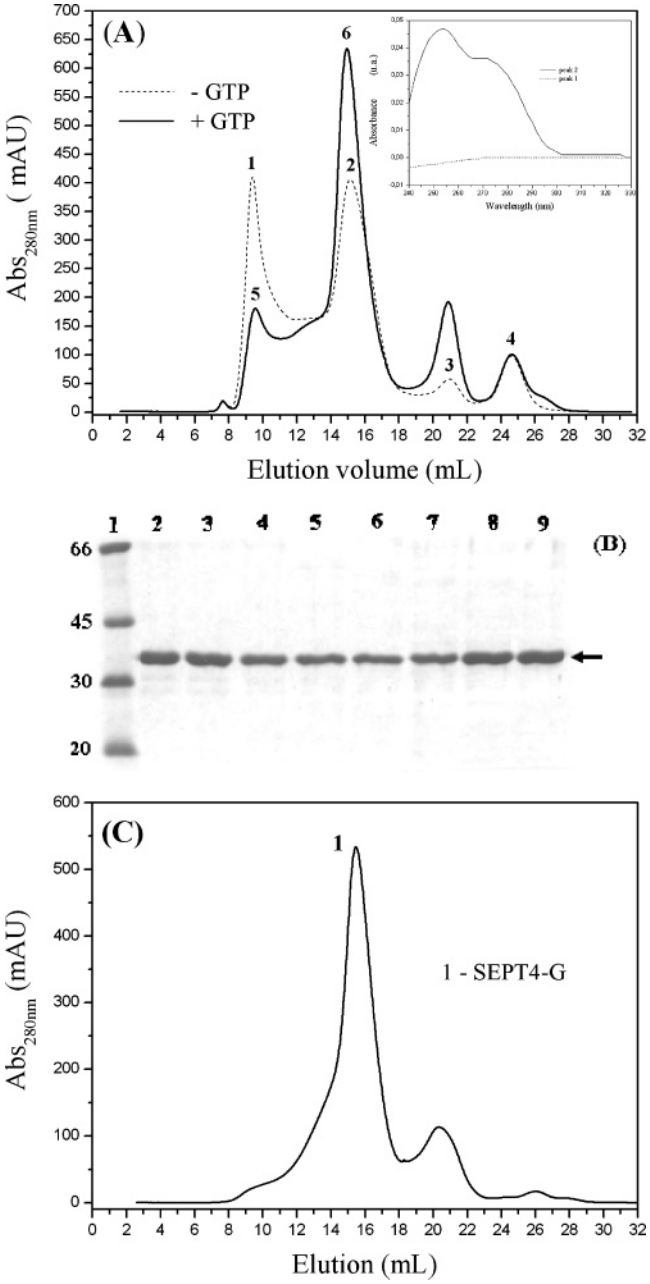

FIGURE 1: Size exclusion chromatography of recombinant SEPT4-G. (A) Size exclusion chromatography of purified SEPT4-G on Superdex-200. Recombinant SEPT4-G purified in the absence of GTP in all the buffers (—). Peak **1** (void) corresponds to aggregated nucleotide-free SEPT4-G, and peak **2** corresponds to nucleotide-bound SEPT4-G which eluted with an apparent molecular mass of ~76 kDa. Peaks **5** and **6** are equivalent to peaks **1** and **2** but for a sample of recombinant SEPT4-G to which GTP had been added to the sample buffer (- - -). The inset shows the nucleotide content recovered from peaks **1** and **2**. (B) Coomassie-stained SDS−PAGE showing SEPT4-G after size exclusion chromatography of the sample purified in the absence of GTP. Lane 1 shows molecular weight standards, and lanes 2−9 correspond to fractions 8−15 mL taken from the column. (C) Recombinant SEPT4-G purified in the presence of GTP in all the buffers (peak **1**).

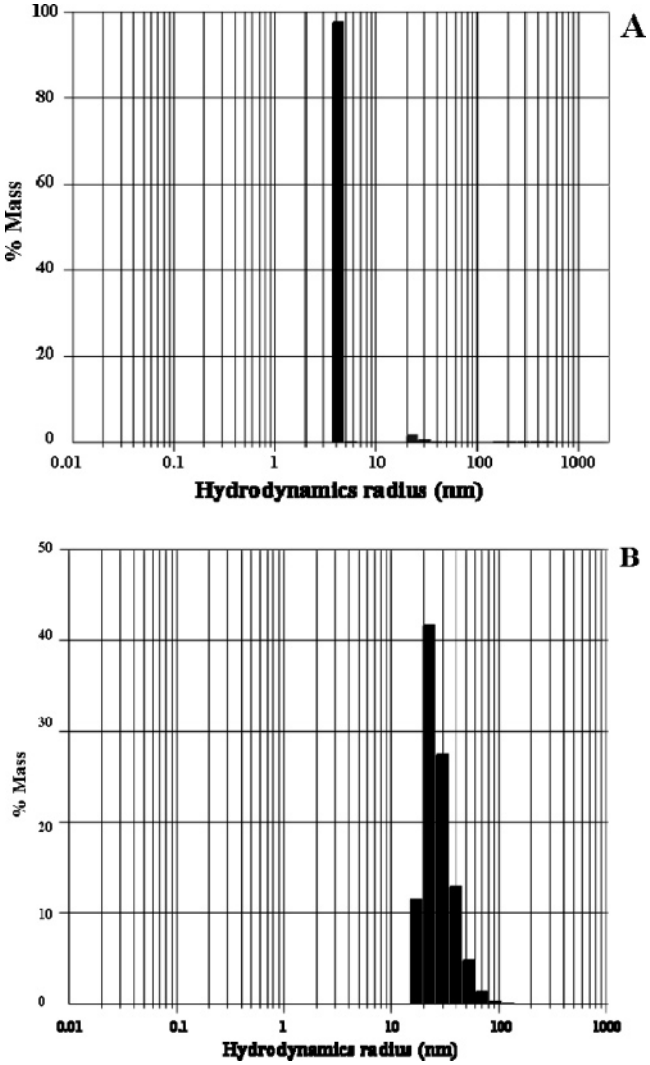

FIGURE 2: Dynamic light scattering. Panels A and B correspond to peaks **2** and **1**, respectively, of Figure 1A.

of the definition of the minima characteristic of α-helix (210 and 221 nm) (Figure 3B). This structural alteration can be seen to correlate with the loss of nucleotide from the molecule since incubation at 24 °C leads to a marked reduction in nucleotide content (Figure 4). On the other hand, when the protein is incubated at temperatures below the transition temperature (4 and 18 °C), nucleotide remains firmly bound as demonstrated by the absence of the typical nucleotide spectrum in the filtrate.

The CD spectrum becomes constant once more between 30 and 42 °C, as evidenced by the intensity of the negative minimum at 221 nm, suggesting the appearance of an intermediate structure within this temperature range (Figure 3B). The profile of the CD spectrum of this intermediate is characteristic of a greater relative content of β-structure, as corroborated by spectral deconvolution (15% α-helix, 35% β-strand, and 50% turns and irregular structures). Above 42 °C, there is a progressive loss of regular secondary structure, and over time, the protein precipitates in a temperature-dependent fashion.

The structural alteration observed by circular dichroism from 22 to 30 °C is accompanied by an increase in the level of binding of ANS to the protein (Figure 5). ANS is an extrinsic fluorescent probe which is sensitive to conformational changes because it undergoes a large increase in the fluorescence quantum yield when bound to proteins (*32*, *33*). ANS is known to bind to hydrophobic surfaces, and the results shown in Figure 5 therefore indicate that the observed conformational change involves the exposure of such residues (*32*, *34*). However, when the temperature is further increased

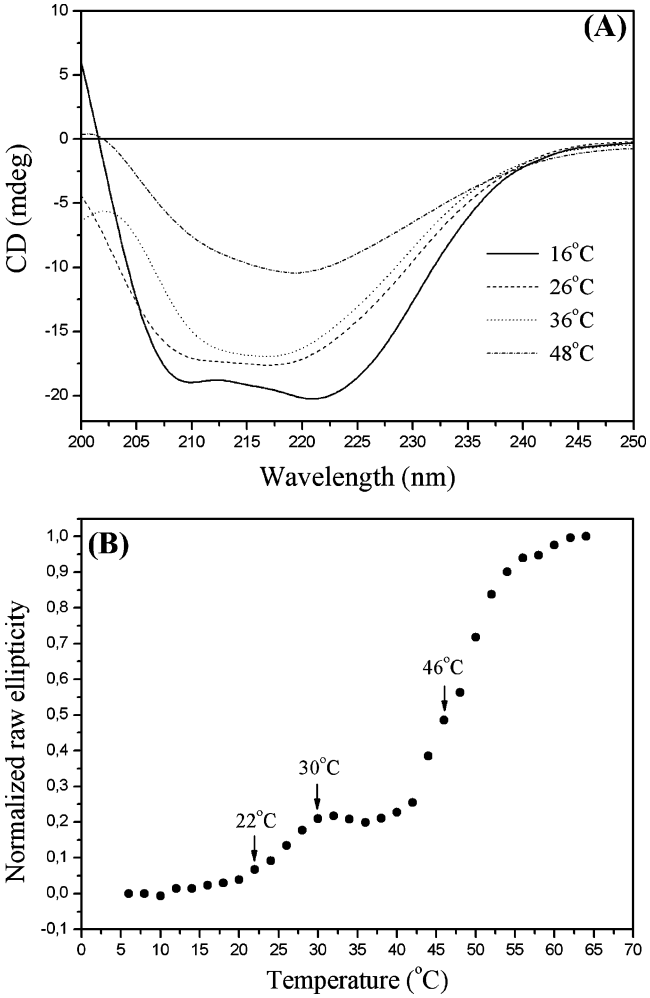

FIGURE 3: Thermal unfolding of human SEPT4-G. (A) CD spectra of the recombinant SEPT4-G (purified with GTP in the lysis buffer) at 16, 26, 36, and 48 °C. The SEPT4-G concentration was approximately 9 μM in 25 mM Tris-HCl, 20 mM NaCl, 0.1 mM EDTA, 5% glycerol buffer (pH 7.8). (B) Thermal denaturation of SEPT4-G was monitored by measuring the ellipticity at 221 nm as a function of temperature.

to values above 30 °C, a marked decay in the fluorescence signal was observed (Figure 5B), implying a reduction in the affinity of the dye at higher temperatures, presumably due to the occlusion of the hydrophobic surfaces. Thus, while the CD spectrum remains constant between 30 and 42 °C, there is a significant decrease in the ANS fluorescence, which returns to approximately its original level, suggesting that the occlusion of hydrophobic regions of the molecule is not accompanied by any significant alteration to its secondary structure. However, the results of ANS binding indicate that the intermediate, which is rich in β-structure, continues to undergo further structural alterations within this temperature range. To investigate the hypothesis that this was due to some form of protein aggregation, a series of additional studies was performed.

Characterizing the Tertiary Structural Changes of SEPT4-G upon Heat Treatment. Right-angle light scattering has been used for studying the polymerization of filament-forming proteins. It has been shown that the intensity of scattered light is linear relative to polymer mass and that this relationship is largely independent of filament length (*35*, *36*). When SEPT4-G was maintained at temperatures between 6 and 28 °C, the level of scattered light remained stable

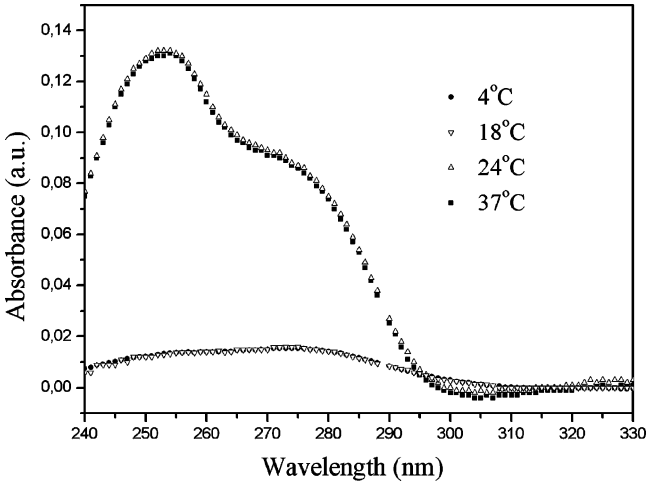

FIGURE 4: Nucleotide release. Absorption spectrum from the filtrate after incubation of SEPT4-G for 90 min at different temperatures followed by centrifugation. At 6 and 18 °C, there is no evidence of release of a nucleotide from the protein, while at 24 and 37 °C, this can be clearly observed from the characteristic absorption spectrum.

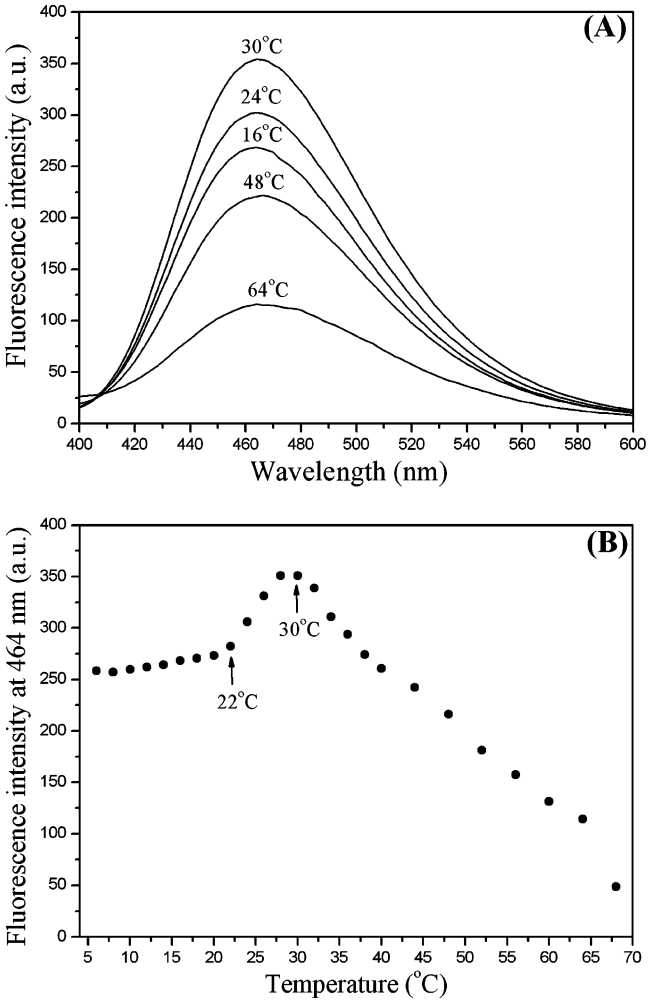

FIGURE 5: ANS fluorescence assay. (A) ANS fluorescence spectra at 16, 24, 30, 48, and 64 °C. (B) Temperature dependence of the ANS fluorescence induced by SEPT4-G as monitored using the fluorescence emission at 464 nm. At temperatures above 30 °C, the fluorescence signal decreases markedly with increasing temperatures.

for the entire duration of the experiment over a wide range of concentrations (1−15 μM). Figure 6 shows the result at

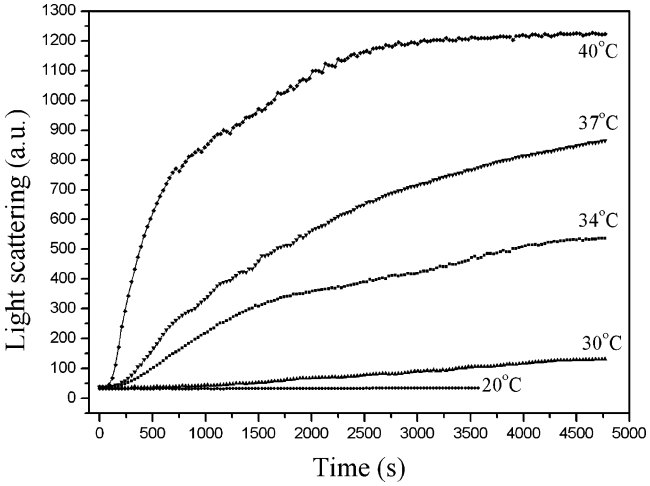

FIGURE 6: Right-angle light scattering. The scattered intensity at 350 nm from SEPT4-G was monitored at 20, 30, 34, 37, and 40 °C.

20 °C. However, incubation of SEPT4-G at temperatures above 30 °C resulted in a rapid increase in light scattering after an initial lag phase. This suggests a temperature-dependent formation of larger particles in solution. However, within the studied temperature range (up to 40 °C) and at the protein concentrations used here, there was no evidence of protein precipitation, and the solutions remained transparent at the end of the experiments.

The rate at which the aggregates form is temperature-dependent and begins around 30 °C, which corresponds to the temperature at which the ANS dye starts to be released from the protein and the intermediate is observed in the CD spectra. This suggests that the occlusion of hydrophobic sites implied by the loss of ANS fluorescence may be due to the formation of large aggregates, leading to the exclusion of the dye. Over time, the light scattering tends toward a maximum value at which the aggregate concentration remained constant over time. This can be clearly seen in the case of the measurements taken at 40 °C.

SEPT4-G Forms Amyloid-like Aggregates upon Heat Treatment within the Same Temperature Range where the Intermediate Species Accumulates. To characterize the nature of the aggregates, the fluorescence probe ThT was employed as was staining with Congo red. ThT is a fluorophore widely used to detect amyloid structure in proteins and usually does not bind to amorphous aggregates. ThT has a limited capacity to bind to SEPT4-G at room temperature (<28 °C). However, the fluorescence signal is observed to increase in a sigmoid-like fashion at temperatures between 30 and 40 °C, indicating that direct interaction with the protein is taking place (Figure 7). In the case of the measurements taken at 40 °C, the plateau could be clearly seen and was reached after approximately 1000 s.

This interaction strongly suggests that the aggregates described above are amyloid-like and therefore not amorphous in nature. The temperature interval which corresponds to a maximum in ThT fluorescence corresponds to that over which the intermediate was observed using CD spectroscopy, suggesting a direct relationship between ThT binding (and therefore amyloid production) and the existence of the structural intermediate. Furthermore, within this temperature range, the protein has already lost its bound nucleotide,

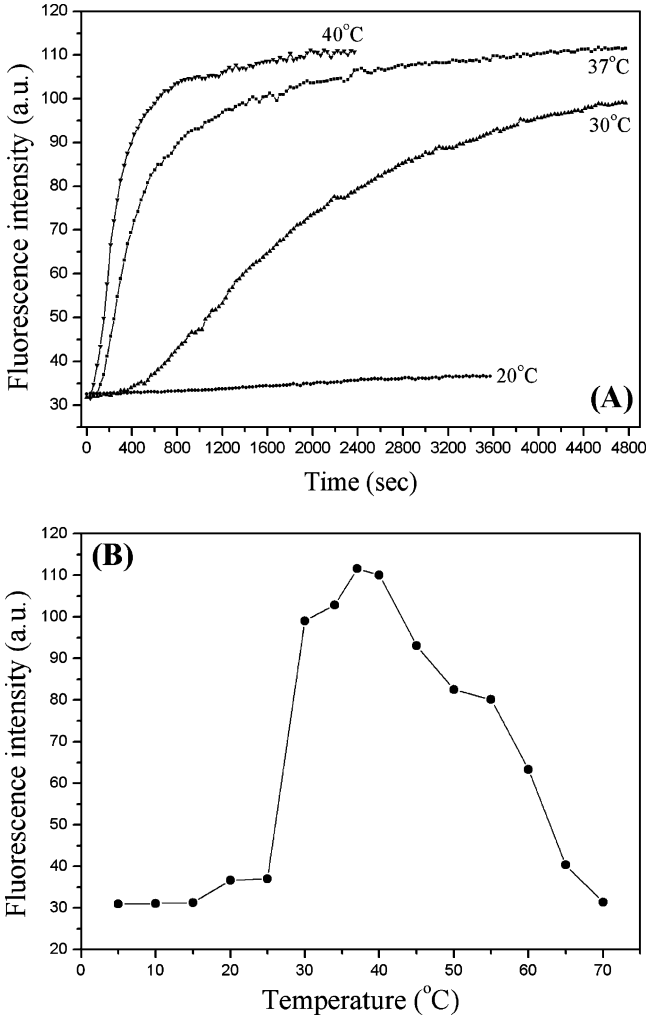

FIGURE 7: ThT fluorescence assay. (A) Fluorescence emission from ThT in the presence of SEPT4-G as a function of time at different temperatures. (B) Fluorescence intensity from ThT after incubation for 60 min in the presence of SEPT4-G at different temperatures. ThT has a weak capacity to bind to SEPT4-G at temperatures below 28 °C. Between 30 and 42 °C, a marked increase in the magnitude of the fluorescence signal is observed. Incubation in temperatures above 45 °C resulted in a decay in the fluorescence signal, suggesting that amyloid formation from SEPT4-G becomes progressively suppressed when the temperature is increased above 45 °C.

indicating that the amyloid-like fibers are nucleotide-free (Figure 4).

Incubation at temperatures above 45 °C resulted in a decay in the overall fluorescence, suggesting that the extent of amyloid formation from SEPT4-G progressively decreases when the temperature is raised above 45 °C or that this is partially due to the protein beginning to precipitate (Figure 7B). We conclude that the initial formation of a partially folded structure, or intermediate, is necessary for the formation of the amyloid-like structures and that at higher temperatures there is a tendency to form amorphous aggregates which are no longer recognized by ThT (*30*, *37*). A summary of the main results described above is given in Table 1.

Characterizing the Morphology and Size of the Aggregates of SEPT4-G Formed upon Heat Treatment. The aggregates which form at 37 °C bind to Congo red as seen by differential interference contrast microscopy (Figure 8B), supporting the

Table 1: Summary of the Main Results

temperature range (°C)	nucleotide binding	aggregation state	secondary structure	ANS binding	ThT binding
6−20	guanine nucleotide bound	soluble dimer	α/β-secondary structure	weak binding to ANS	weak ThT binding
22−28	loss of nucleotide	soluble	structural transition	strong binding to ANS	weak ThT binding
30−42	nucleotide free	soluble fibers	β-rich intermediate	ANS release	strong ThT binding
>42	nucleotide free	aggregates	denatured over time	ANS free	weak ThT binding

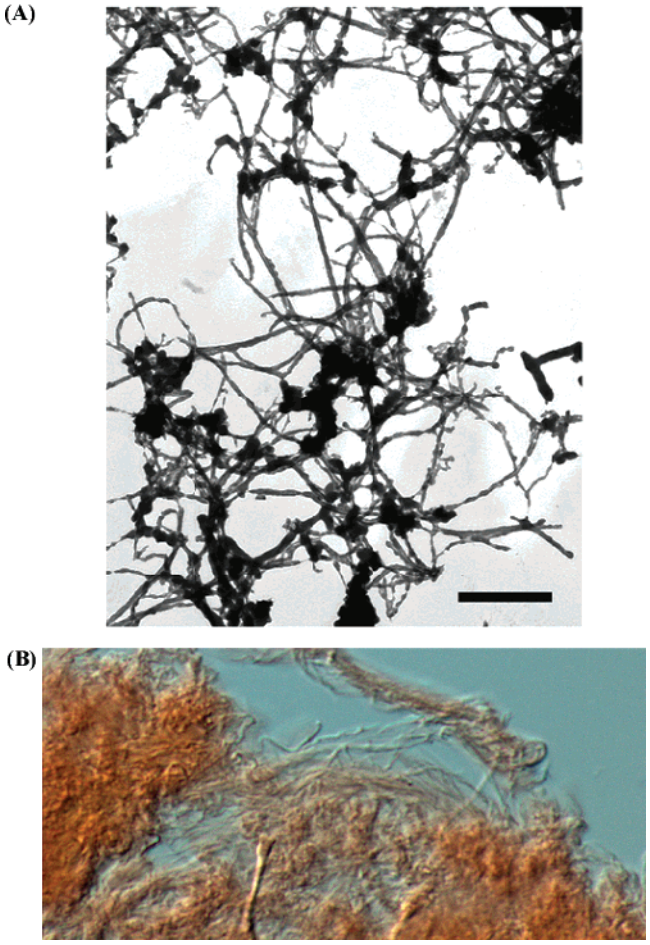

FIGURE 8: (A) Negative stain electron micrograph of SEPT4-G fibrils after incubation for 30 min at 37 °C. The scale bar corresponds to 1000 nm. (B) Difference interferential contrast of an identically treated sample stained with Congo red.

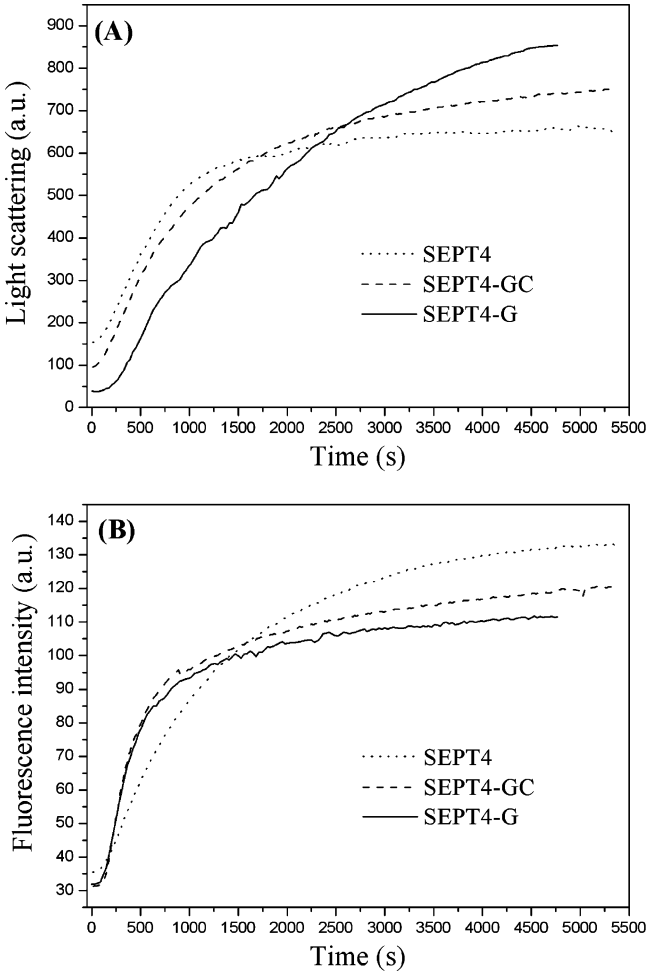

FIGURE 9: Comparison between the aggregation behavior (A) and ThT fluorescence (B) of the whole protein (SEPT4), SEPT4-GC (GTPase domain with the C-terminal domain), and SEPT4-G. The scattered intensity (at 350 nm) and fluorescence emission from ThT (at 482 nm) were monitored at 37 °C as a function of time.

suggestion that they are amyloid-like and the fact that they present only a low birefringence which is not inconsistent with this hypothesis as recently discussed (*37*). These same aggregates were observed via electron microscopy to present a complex network of unbranched fibrils with highly variable diameters (10−40 nm) and lengths up to several micrometers (Figure 8A). Wider fibers often appear to be the results of the superposition of smaller ones.

Progress in the study of the biochemistry and cell biology of septins has been hampered by the apparent instability of most septins when expressed as single recombinant molecules (*4*, *5*). This also explains the current absence of a crystal structure for any septin or domain thereof. A better understanding of septin stability is therefore a hurdle which must be overcome to make significant progress in comprehending the molecular mechanisms which directly associate different septins with specific pathological conditions, such as neoplasia, neuropathology, and infectious diseases (*38*). Toward this goal, here we describe a detailed study of the stability of the principal domain of human SEPT4.

It should be borne in mind that it is reasonable to study the GTPase domain in isolation given that the N-terminal domain is intrinsically unstructured (*27*) and that a protein product including both the GTPase and C-terminal domains together (SEPT-GC) behaves like SEPT4-G alone (*27*). Furthermore, at physiological temperature (37 °C), both the whole septin molecule (SEPT4) and the SEPT4-GC product exhibit aggregation behavior similar to that of SEPT4-G (Figure 9A). Once again, this aggregation is related to the binding of ThT (Figure 9B), suggesting the aggregates to be amyloid-like. These results indicate that the biophysical characterization of the GTPase domain alone reported here is pertinent to the whole molecule. It should be pointed out that by studying the GTPase domain in isolation we have

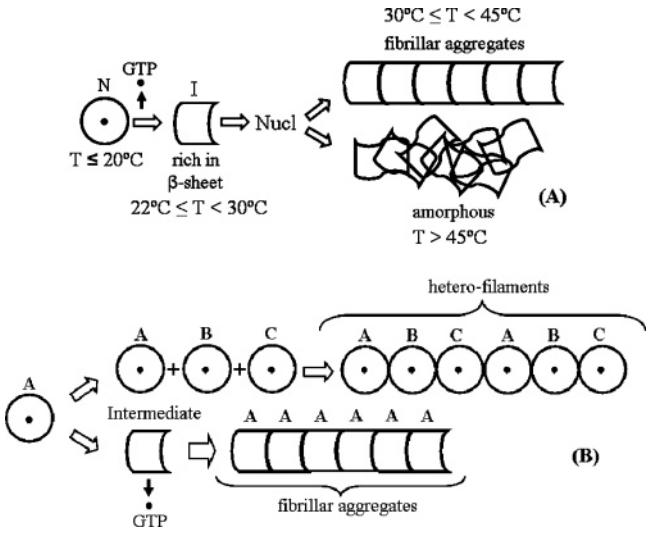

FIGURE 10: Reaction scheme for SEPT4-G unfolding. (A) N and I indicate the native form and intermediate state of SEPT4-G, respectively. Nucl is a presumed nucleation state which may lead to either fibril formation (F) within a defined temperature interval or aggregation. (B) Possible polymerization schemes for septins in general both in vivo and in vitro. A, B, and C are generic names which refer to three different septin molecules. In panels A and B, the ● symbol indicates GTP.

been able to identify a thermal unfolding intermediate which would be difficult, if not impossible, to identify using a multidomain molecule.

The results described above are consistent with a model for amyloid formation by the septin 4 GTPase domain which is summarized in Figure 10A. At temperatures up to around 20 °C, the SEPT4-G domain is stable in solution in its nucleotide-bound dimeric form. As the temperature is increased from 22 to 30 °C, there is an alteration to the secondary structure which is accompanied by the exposure of hydrophobic residues and the loss of guanine nucleotide. From 30 to ~42 °C, a partially unfolded intermediate is observed which is rich in β-structure. Within this temperature range, this intermediate tends to polymerize, forming amyloid-like structures which bind Congo Red and ThT and can be directly visualized by electron microscopy (*37*). On polymerization within this temperature range, there is no observable alteration to the secondary structure; however, the hydrophobic regions exposed during partial unfolding up to 30 °C once more become buried, and ANS is rapidly released from the molecule. At temperatures above 42 °C, further alteration to the secondary structure is observable in the CD spectrum, indicative of further unfolding. This leads to the formation of amorphous protein aggregates, which no longer bind ThT (*37*), and finally results in precipitation.

There has been considerable discussion in the recent literature concerning the formation of both homo- and heteropolymers of septins (*4*, *6*, *7*, *31*, *39*). In vivo studies seem to agree that functional filaments must be composed of more than two different septins, and the majority of in vitro studies show similar results. However, there are at least two reports in the literature of the formation of homopolymers in vitro (*6*, *7*). Although it is not necessarily to be expected that all septins will behave similarly in this respect, the former of these reports has been questioned particularly with respect to the nature of the filaments and their physiological relevance (*31*). Here we provide a possible explanation for the observation of homopolymers, by demonstrating that the GTPase domain of SEPT4 is capable of forming amyloid-like filamentous structures in vitro under well-defined conditions. Indeed, the filaments reported here are considerably wider than those described in vivo in yeast (*1*) and also those observed on coexpression of mammalian septins 2, 6, and 7 in vitro (*4*), both of which are believed to represent functional filaments. The difference between these two polymerization schemes is illustrated in Figure 10B. Our results suggest a need for a critical re-examination of the nature of what have been described as septin filaments in the past, and also for careful attention to the physicochemical conditions used for their observation.

It is intriguing that the amyloids described here are formed rapidly under conditions of temperature and pH which are close to physiological; this raises the possibility that they may have a physiological role rather than being merely an in vitro artifact. If indeed the formation of active filaments requires the presence of different septins [which presumably increase the overall stability of the individual components of the complex (*4*, *5*, *39*)], then polymerization in the form of amyloid may be a means of eliminating a component which happens to be present in excess. Obviously, this would have to be viable under physiological conditions, as observed here. This is consistent with recent ideas which suggest that amyloid-like aggregates may represent a physiological mechanism for detoxifying smaller disease-causing protofilaments (*37*).

A recent report showed that SEPT4 accumulates in cytoplasmic inclusions found in three major synucleinopathies: Parkinson's disease (PD), dementia with Lewy bodies (DLB), and multiple-system atrophy (MSA) (*19*). Furthermore, one report suggests that SEPT4, together with SEPT1 and SEPT2, may also be associated with neurofibrillary tangles and other pathological features of senile plaques in Alzheimer's disease (*18*). However, the use of monoclonal antibodies against a GST−SEPT4 fusion protein (*40*) showed no significant reaction to disease-related pathological features in human specimens obtained from both Parkinson's and Alzheimer's patients (M. Tanaka et al., unpublished data). Therefore, whatever the exact role of SEPT4 in different disease processes, a need for a better understanding of its biophysical behavior, including its aggregation properties, is clearly needed.

The data provided here raise important questions with respect to the possible association of SEPT4 with neurodegenerative diseases. At the very least, they suggest a possible mechanism for the association of partially unfolded SEPT4 with the pathological processes with which it has been suggested to be associated.

In this study, we describe the first report of amyloid formation by any septin and have therefore gone some way toward establishing methodologies for future research. Such studies on the biochemical and biophysical properties and physiological functions of septins should provide important insights into the common mechanism underlying diverse neurodegenerative disorders.

ACKNOWLEDGMENT

We thank Suzana Sculaccio and Derminda I. de Moraes for technical assistance and José Manuel Andreu Morales

for carefully reading the manuscript. We express our gratitude to Dr. Ulisses Lins and Dr. Thais Souto Padron (Instituto de Microbiologia) and Prof. Paulo de Góes (Federal University of Rio de Janeiro) for access to their Zeiss Axioplan 2 epifluorescence microscope and the Morgagni transmission electron microscope.

REFERENCES

1. Frazier, J. A., Wong, M. L., Longtine, M. S., Pringle, J. R., Mann, M., Mitchison, T. J., and Field, C. (1998) Polymerization of purified yeast septins: Evidence that organized filament arrays may not be required for septin function, *J. Cell Biol. 143*, 737−749.
2. Field, C. M., al-Awar, O., Rosenblatt, J., Wong, M. L., Alberts, D., and Mitchison, T. J. (1996) A purified *Drosophila* septin complex forms filaments and exhibits GTPase activity, *J. Cell Biol. 133*, 605−616.
3. Hsu, S. C., Hazuka, C. D., Roth, R., Foletti, D. L., Heuser, J., and Scheller, R. H. (1998) Subunit composition, protein interactions, and structures of the mammalian brain sec6/8 complex and septin filaments, *Neuron 20*, 1111−1122.
4. Sheffield, P. J., Oliver, C. J., Kremer, B. E., Sheng, S., Shao, Z., and Macara, I. G. (2003) Borg/Septin interactions and the assembly of mammalian septin heterodimers, trimers, and filaments, *J. Biol. Chem. 278*, 3483−3488.
5. Kinoshita, M., Field, C. M., Coughlin, M. L., Straight, A. F., and Mitchison, T. J. (2002) Self- and actin-templated assembly of mammalian septins, *Dev. Cell 3*, 791−802.
6. Mendoza, M., Hyman, A. A., and Glotzer, M. (2002) GTP binding induces filament assembly of a recombinant septin, *Curr. Biol. 12*, 1858−1863.
7. Huang, Y., Surka, M. C., Reynaud, D., Pace-Asciak, C., and Trimble, W. S. (2006) GTP binding and hydrolysis of human septin2, *FEBS J. 273*, 3248−3260.
8. Macara, I. G., Baldarelli, R., Field, C. M., Glotzer, M., Hayashi, Y., Hsu, S. C., Kennedy, M. B., Kinoshita, M., Longtine, M., Low, C., Maltais, L. J., McKenzie, L., Mitchison, T. J., Nishikawa, T., Noda, M., Petty, E. M., Peifer, M., Pringle, J. R., Robinson, P. J., Roth, D., Russell, S. E., Stuhlmann, H., Tanaka, M., Tanaka, T., Trimble, W. S., Ware, J., Zeleznik-Le, N. J., and Zieger, B. (2002) Mammalian septins nomenclature, *Mol. Biol. Cell 13*, 4111−4113.
9. Kartmann, B., and Roth, D. (2001) Novel roles for mammalian septins: From vesicle trafficking to oncogenesis, *J. Cell Sci. 114*, 839−844.
10. Martínez, C., Sanjuan, M. A., Dent, J. A., Karlsson, L., and Ware, J. (2004) Human septin-septin interactions as a prerequisite for targeting septin complexes in the cytosol, *Biochem. J. 382*, 783−791.
11. Field, C. M., and Kellogg, D. (1999) Septins: Structural polymers or signaling GTPases, *Trends Cell Biol. 9*, 387−394.
12. Zhang, J., Kong, C., Xie, H., McPherson, P. S., Grinstein, S., and Trimble, W. S. (1999) Phosphatidylinositol polyphosphate binding to the mammalian septin H5 is modulated by GTP, *Curr. Biol. 9*, 1458−1467.
13. Hillebrand, S., Garcia, W., Cantú, M. D., Araújo, A. P. U., Tanaka, M., Tanaka, T., Garratt, R. C., and Carrilho, E. (2005) In vitro monitoring of GTPase activity and enzyme kinetics studies using capillary electrophoresis, *Anal. Bioanal. Chem. 383*, 92−97.
14. Tanaka, M., Tanaka, T., Kijima, H., Itoh, J., Matsuda, T., Hori, S., and Yamamoto, M. (2001) Characterization of tissue- and cell-type-specific expression of a novel human septin family gene, Bradeion, *Biochem. Biophys. Res. Commun. 286*, 547−553.
15. Xie, H., Surka, M., Howard, J., and Trimble, W. S. (1999) Characterization of the mammalian septin H5: Distinct patterns of cytoskeletal and membrane association from other septin proteins, *Cell Motil. Cytoskeleton 43*, 52−62.
16. Larisch, S., Youngsuk, Y., Lotan, R., Kerner, H., Eimerl, S., Parks, W. T., Gottfried, Y., Reffey, S. B., Caestecker, M. P., Danielpour, D., Book-Melamed, N., Timberg, R., Duckett, C. S., Lechleider, R. J., Steller, H., Orly, J., Kim, S., and Roberts, A. B. (2000) A novel mitochondrial septin-like protein, ARTS, mediates apoptosis dependent on its P-loop motif, *Nat. Cell Biol. 2*, 915−921.
17. Tanaka, T., Kijima, H., Itoh, J., Matsuda, T., and Tanaka, T. (2002) Impaired expression of a human septin family gene Bradeion inhibits the growth and tumorigenesis of colorectal cancer *in vitro* and *in vivo*, *Cancer Gene Ther. 9*, 483−488.
18. Kinoshita, A., Kinoshita, M., Akiyama, H., Tomimoto, H., Akiguchi, I., Kumar, S., Noda, M., and Kimura, J. (1998) Identification of septins in neurofibrillary tangles in Alzheimer's disease, *Am. J. Pathol. 153*, 1551−1560.
19. Ihara, M., Tomimoto, H., Kitayama, H., Morioka, Y., Akigunchi, I., Shibasaki, H., Noda, M., and Kinoshita, M. (2003) Association of the cytoskeletal GTP-binding protein Sept4/H5 with cytoplasmatic inclusions found in Parkinson's disease and others synucleinopathies, *J. Biol. Chem. 278*, 24095−24012.
20. DiFiglia, M., Sapp, E., Chase, K. O., Davies, S. W., Bates, G. P., Vonsattel, J. P., and Aronin, N. (1997) Aggregation of huntingtin in neuronal intranuclear inclusions and dystrophic neurites in brain, *Science 277*, 1990−1993.
21. Selkoe, D. J. (2004) Cell biology of protein misfolding: The examples of Alzheimer's and Parkinson's diseases, *Nat. Cell Biol. 6*, 1054−1061.
22. Ross, C. A., and Poirier, M. A. (2004) Protein aggregation and neurodegenerative disease, *Nat. Med. 10*, S10−S17.
23. Dobson, C. M. (2003) Protein folding and misfolding, *Nature 426*, 884−890.
24. Ross, C. A., and Margolis, R. L. (2005) Neurogenetics: Insights into degenerative diseases and approaches to schizophrenia, *Clin. Neurosci. Res. 5*, 3−14.
25. Makin, O. S., and Serpell, L. C. (2005) Structures for amyloid fibrils, *FEBS J. 272*, 5950−5961.
26. Sunde, M., and Blake, C. F. (1998) From the globular to the fibrous state: Protein structure and structural conversion in amyloid formation, *Q. Rev. Biophys. 31*, 1−39.
27. Garcia, W., Araújo, A. P. U., Neto, M. O., Ballestero, M. R. M., Polikarpov, I., Tanaka, M., Tanaka, T., and Garratt, R. C. (2006) Dissection of a human Septin: Definition and characterization of distinct domains within human SEPT4, *Biochemistry 45*, 13918−13931.
28. Gill, S. C., and von Hippel, P. H. (1989) Calculation of proteins extinction coefficients from amino acid sequence data, *Anal. Biochem. 182*, 319−326.
29. Seckler, R., Wu, G. M., and Timasheff, S. N. (1990) Interactions of tubulin with guanylyl-(β-γ-methylene)diphosphate, *J. Biol. Chem. 265*, 7655−7661.
30. Edmonds, B. T., Bell, A., Wyckoff, J., Condeelis, J., and Leyh, T. S. (1998) The effect of F-actin on the binding and hydrolysis of guanine nucleotide by *Dictyostelium* elongation factor 1A, *J. Biol. Chem. 273*, 10288−10295.
31. Mitchison, T., and Field, C. M. (2002) Cytoskeleton: What does GTP do for dispatch septins? *Curr. Biol. 12*, R788−R790.
32. Semisotnov, G. V., Rodionova, A. N., Kutyshenko, V. P., Ebert, B., Blanck, J., and Ptitsyn, O. B. (1987) Sequential mechanism of refolding of carbonic anhydrase-b, *FEBS Lett. 224*, 9−13.
33. Srisailam, S., Wang, H. M., Kumar, T. K. S., Rajalingam, D., Sivaraja, V., Sheu, H. S., Chang, Y. C., and Yu, C. (2002) Amyloid-like fibril formation in an all β-barrel protein involves the formation of partially structured intermediate(s), *J. Biol. Chem. 277*, 19027−19036.
34. Fandrich, M., Forge, V., Buder, K., Kittler, M., Dobson, C. M., and Diekmann, S. (2003) Myoglobin forms amyloid fibrils by association of unfolded polypeptide segments, *Proc. Natl. Acad. Sci. U.S.A. 100*, 15463−15468.
35. Kang, F., Purich, D. L., and Southwick, F. S. (1999) Profilin promotes barbed-end actin filament assembly without lowering the critical concentration, *J. Biol. Chem. 274*, 36963−36972.
36. Romberg, L., Simon, M., and Erickson, H. P. (2001) Polymerization of FtsZ, a bacterial homolog of tubulin, is assembly cooperative, *J. Biol. Chem. 276*, 11743−11753.
37. Chiti, F., and Dobson, C. M. (2006) Protein misfolding, functional amyloid, and human disease, *Annu. Rev. Biochem. 75*, 333−366.
38. Hall, P., and Russell, S. (2004) The pathobiology of the septin gene family, *J. Pathol. 204*, 489−505.
39. Low, C., and Macara, I. G. (2006) Structural analysis of septin 2, 6 and 7 complexes, *J. Biol. Chem. 281*, 30697−30706.
40. Tanaka, M., Tanaka, T., Matsuzaki, S., Seto, Y., Matsuda, T., Komori, K., Itoh, J., Kijima, H., Tamai, K., Shibayama, M., Hashimoto, Y., Nakazawa, H., and Toma, H. (2003) Rapid and quantitative detection of human septin family Bradeion as a practical diagnostic method of colorectal and urologic cancers, *Med. Sci. Monit. 9*, CR2−CR9.

BI700702W